

CHARACTERISATION OF STRUCTURAL RELAXATION PHENOMENA IN POLYMERIC MATERIALS FROM THERMAL ANALYSIS INVESTIGATIONS

Allisson Saiter*, H. Couderc and J. Grenet

Laboratoire PBM, UMR 6522, LECAP, Institut des Matériaux de Rouen, Faculté des Sciences, Avenue de l'Université BP 12 76801 Saint Etienne du Rouvray, France

Measurements have been performed on poly(ethylene terephthalate)glycol/montmorillonite nanocomposites with different filler contents using differential scanning calorimetry (DSC) and temperature modulated differential scanning calorimetry (TMDSC). According to the strong-fragile concept proposed by Angell, we have determined the values of the fragility index m . In a second time, we have calculated the average size of a cooperative rearranging region (CRR) $z(T_g)$ at the glass transition according to the definition proposed by Solonov. However, $z(T_g)$ is a dimensionless quantity and then only allows a comparative study between different samples. To calculate the average number of monomer units by CRR noted N_α , we have used the method developed by Donth. The results show that the presence of montmorillonite in PET_g matrice implies modifications on structural relaxation phenomena. Furthermore, we have shown that $z(T_g)$ and N_α values have the same evolution in function of filler content.

Keywords: CRR, DSC, fragility, nanocomposites, TMDSC

Introduction

Structural relaxation is a general phenomenon occurring when a glass is maintained at a temperature T_a below its glass transition temperature T_g . It is generally called physical ageing [1]. Consequently, ageing implies the variation with time of many glass properties, such as the enthalpy variations presented in Fig. 1. The liquid-glass transition is experimentally characterised by the glass transition temperature T_g , often defined either as the temperature where the equilibrium liquid has a viscosity equal to 10^{12} Pa s [2], or as the temperature where the average relaxation time in the equilibrium liquid is equal to 100 s. From some data concerning solutions and polymers,

Angell [2] has observed that the variations of the viscosity η (or relaxation time τ) with the temperature, and more exactly with the normalised reduced quantity T_g/T , are included between two limits. An Arrhenius law describes the first limit, leading to the so-called ‘strong’ glass-forming liquid behaviour, while a Vogel–Tamman–Fulcher law describes the second, leading to the ‘fragile’ glass-forming liquid behaviour. Because all glass-forming liquids are located between these two limits, Ngai *et al.* [3] have proposed to characterize the behaviour by the slope of $\log_{10}\tau$ vs. T_g/T curve at the glass transition. This slope, called the fragility index m , is defined by:

$$m = \left. \frac{d \log_{10} \tau}{dT_g / T} \right|_{T=T_g} \quad (1)$$

From DSC investigations the calculation of m requires the knowledge of the relaxation time dependence over T . The Tool–Narayanaswamy–Moynihan expression [4–6] is widely used for glassy materials:

$$\tau = \tau_0 \exp\left(\frac{x \Delta h^*}{RT}\right) \exp\left[\frac{(1-x)\Delta h^*}{RT_f}\right] \quad (2)$$

with τ_0 the pre-exponential factor, x the non-linearity parameter, Δh^* the apparent activation enthalpy, R the perfect gas constant, and T_f , the fictive temperature. The fictive temperature concept was defined by Tool [4, 7] to describe the thermodynamic state of glasses. Indeed, he has shown from dilatometric mea-

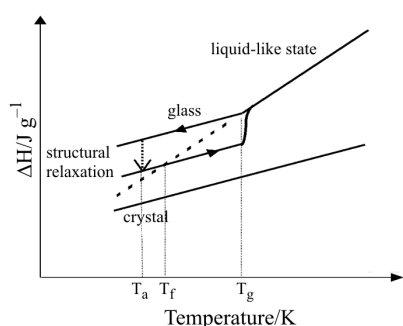


Fig. 1 Enthalpic variations with temperature for a glass forming system and a crystal. The dotted arrow indicates the enthalpic variations during the structural relaxation at T_a (the ageing temperature). This figure also shows the fictive temperature T_f and the glass transition temperature T_g

* Author for correspondence: allison.saiter@univ-rouen.fr

surements on glasses, that the structural relaxation can not be described only by a relaxation time depending on temperature, but also depending on the instantaneous glass structure. This instantaneous structure is given by T_f depending on the cooling rate: the greater the cooling rate, the higher the fictive temperature. The relaxation time at T_f and the cooling rate being linked by the relationship $\tau(T_f)q^- = \text{const.}$ [8, 9], the apparent activation energy could be obtained from the variations of T_f with q^- :

$$\frac{\Delta h^*}{R} = \frac{d(\ln|q^-|)}{d(1/T_f)} \quad (3)$$

Then using Eqs (1) and (2), it is easy to show that the fragility index m can be determined from DSC investigations by:

$$m = \frac{\Delta h^*}{RT_g \ln 10} \quad (4)$$

Many studies show that the determination of the fragility index allows to characterize and to compare different glass-forming liquids between them [10, 11].

The relaxation process in the glassy state is a cooperative phenomenon and the molecule motion depends on neighbour's motions [12]: The rearranging movement of one structural unit is only possible if a certain number of neighbouring structural units is also moved. Adam and Gibbs [13] introduced the notion of cooperative rearranging region (CRR) defined as a subsystem, which can rearrange its configurations into another, independently of its environment upon a sufficient thermal fluctuation. Solunov characterized the average size of a CRR by the quantity $z(T)$ [14] corresponding to the average number of structural units that relax together to cross from one configuration to another. However these structural units are not clearly defined: are they monomers, monomer segments, polymeric chains?

$z(T)$ can be determined from the following equation [14]:

$$z(T) = \frac{T}{T - T_k} \quad (5)$$

where T_k is the Kauzmann temperature. Then, the average size of a CRR at the glass transition can be evaluated from:

$$z(T_g) = \frac{T_g}{T_g - T_k} \quad (6)$$

In this work, we propose to characterize the structural relaxation phenomena by T_g , m and $z(T_g)$ determinations, from DSC and TMDSC investigations on PET_g/montmorillonite nanocomposites, in

order to see if the montmorillonite (MMT) introduction in PET_g matrice influences the structural relaxation phenomena. The use of PET_g matrice has been motivated because it is an amorphous thermoplastic. Indeed, with a semi-crystalline matrice, montmorillonite sheets would behave as nucleation centres [15]. The choice of polymer/clay nanocomposites has been motivated by the fact that these materials present a greater interest for researcher community. Indeed, they markedly exhibit improved mechanical, thermal, optical and physico-chemical properties when compared with the pure polymer and usual composites as firstly demonstrated by Kojima *et al.* [16].

Experimental

Materials and methods

Amorphous PET_g was obtained from Eastman Chemical Company. Cloisite 15A was supplied by Southern Clay. Layered silicate was treated with dimethyl dihydrogenated tallow quaternary ammonium chloride (2M2HT). Montmorillonite C15A has organic modifier concentrations of 95 meq/100 g [17]. PET_g pellets were dried 14 h in a vacuum oven at 80°C. Master batch (15 mass%) was prepared on a Thermo-prism co-rotating twin-screw extruder of 16 mm screw diameter and a L/D ratio of 24/1. The medium/high shear screw design with good dispersion characteristic was chosen for the master batch preparation. Master batch was diluted to individual compositions (1, 2, 3 and 5 mass%) on the same twin-screw extruder. Nanocomposites were processed within a temperature range of 215 to 250°C. PET_g nanocomposite films of 0.254 mm thickness were prepared on a Thermo Haake Polydrive single screw extruder with a film die attached. All samples were dried overnight in a vacuum oven at 80°C prior to every run. Films were collected on a chilled roll system set at temperature of 20°C. For more clarity, the different samples will be noted pure PET_g, PET_g-1% MMT, PET_g-2% MMT, PET_g-3% MMT, PET_g-5% MMT in this paper.

We have previously analysed these different samples by X-ray diffraction to characterise the microstructure. We used a D8 Advance from Bruker AXS. The source wavelength is $\lambda=1.78897$ Å (α line of Co). The sample was placed in Bragg-Brentano configuration. The 2θ diffraction diagrams were determined between 2 and 60°. The samples were studied in the same experimental conditions and held on a silicon substrate, which do not exhibit any diffraction line in the considered domain. The diffraction peaks were fitted by Lorentzian equations. The sample diffractograms are presented on Fig. 2. The

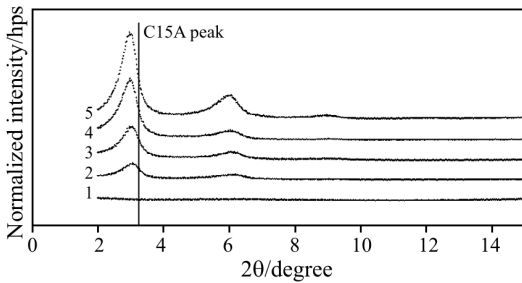


Fig. 2 X-ray diffractograms of 1 – pure PET_g and 2 – 1, 3 – 2, 4 – 3, 5 – 5 mass% content nanocomposites and C15A basal distance representation

containing MMT samples show multiple diffraction peaks with intensity increasing with the filler content, normally due to the diffracting object content increase. The first diffraction peak corresponds to the basal spacing. Notice that for C15A, the basal spacing is equal to 3.15 nm and this value is represented by the vertical line on the Fig. 2. The basal spacing is constant for all the nanocomposites and is equal to 3.5 nm. So, the structure is intercalated or semi-exfoliated. Moreover, the ratio between the inter-reticular distances d_2/d_1 , d_3/d_1 and d_4/d_1 are respectively equal to 0.5, 0.33 and 0.25. That is to say that the multiple diffraction peaks originate from the multiple diffractions in the samples (order of 2, 3 and 4 in the Bragg law). So, the diffraction diagrams can be summarised into one characteristic diffraction between the MMT sheets.

Classical DSC experiments were conducted on Thermal Analysis Instrument heat flow calorimeter (DSC 2920 CE), coupled with a liquid nitrogen cooling system. The apparatus was calibrated by indium. All parameters defined in relationship (2) can be determined from this technique, more particularly by using the Moynihan method [2] to determine the fictive temperature T_f and the apparent activation energy Δh^* . Practically, the sample is heated to 373 K, a temperature upper than T_g in order to erase thermal history. Then, the sample is cooled to 318 K (temperature below T_g) at variable cooling rates q^- , and the measurement is performed during a ramp with constant heating rate $q^+ = 10 \text{ K min}^{-1}$ to 373 K. The sample undergoes several

such thermal cycles with $|q^-| = 0.3, 0.5, 1, 2, 5, 8, 10, 15$ and 20 K min^{-1} . The variations of the fictive temperature T_f with cooling rates q^- allow the determination of the apparent activation energy Δh^* according to Eq. (3). The fictive temperature T_f is equal to T_g when $|q^-| = q^+ = 10 \text{ K min}^{-1}$.

Specific heat capacities of the glass (C_{pglass}) and the liquid like state (C_{pliquid}) at constant pressure, and ΔC_p values have been determined from temperature modulated differential scanning calorimetry (TMDSC) performed on the same apparatus (DSC 2920 CE). The specific heat capacities were measured using sapphire as a reference. The sample masses have been chosen to be similar of the sapphire sample mass, i.e. approximately 20 mg. An oscillation amplitude of 1 K and an oscillation period of 60 s with a heating rate of 5 K min^{-1} were used. Practically, the sample is heated from 303 up to 393 K, final temperature above the glass transition in order to erase the thermal history. Then, the sample is cooled to 303 K at a cooling rate $|q^-| = 5 \text{ K min}^{-1}$, and the measurement is performed during a ramp at constant heating rate of 5 K min^{-1} to 393 K. Before any discussion, the raw data were normalized in relation to the polymer content.

Results and discussion

Figures 3–5 give examples of curves obtained by DSC on pure PET_g, PET_g–2% MMT and PET_g–5% MMT respectively, for different cooling rates going from 20 to 0.3 K min^{-1} . Whatever the sample, the endothermic peak observed at the glass transition and characteristic of structural relaxation phenomena increases with decreasing cooling rate. These variations with q^- allow to determine the apparent activation energy Δh^* and the fragility index m as explained above. Table 1 reports the values of the glass transition temperature T_g determined for $q^+ = |q^-| = 10 \text{ K min}^{-1}$ and the values of the specific heat capacity jump at the glass transition $\Delta C_p(T_g)$ calculated from the raw curves normalized in function of the polymer content. In regard to these different values and uncertainties, we can conclude that there is no significant evolution for polymer

Table 1 Values of parameters determined from DSC experiments

	Pure PET _g	PET _g –1% MMT	PET _g –2% MMT	PET _g –3% MMT	PET _g –5% MMT
T_g/K	352.8 ± 0.5	351.8 ± 0.5	352.1 ± 0.5	350.9 ± 0.5	349.5 ± 0.5
$\Delta C_p(T_g)/\text{J K}^{-1} \text{ g}^{-1}$	0.27 ± 0.01	0.26 ± 0.01	0.24 ± 0.01	0.26 ± 0.01	0.26 ± 0.01
$(\Delta h^*/R)/\text{kK}$	99.8 ± 10	107.9 ± 11	97.6 ± 10	76.8 ± 8	86 ± 9
m	124 ± 12	134 ± 13	121 ± 12	96 ± 10	108 ± 11
$z(T_g)$	8 ± 1	8 ± 1	7.5 ± 1	6 ± 1	7 ± 1

T_g – the glass transition temperature at $q^+ = q^- = 10 \text{ K min}^{-1}$, $\Delta C_p(T_g)$ – the specific heat capacity jump at the glass transition, $\Delta h^*/R$ – the apparent activation energy according to Eq. (3), m – the fragility index according to Eq. (4), $z(T_g)$ – the average size of CRR according to Eq. (7). The uncertainty for each value corresponds to nominal error

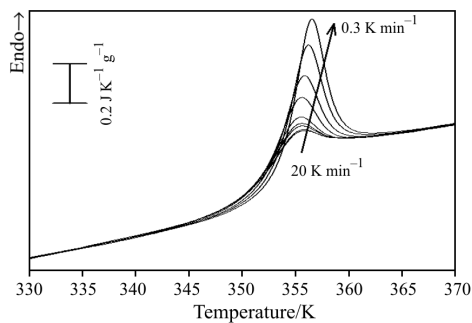


Fig. 3 Pure PET_g: DSC heating curves obtained after various cooling rates (from 20 to 0.3 K min⁻¹ as shown by the arrow), the heating rate is $q^+ = 10$ K min⁻¹

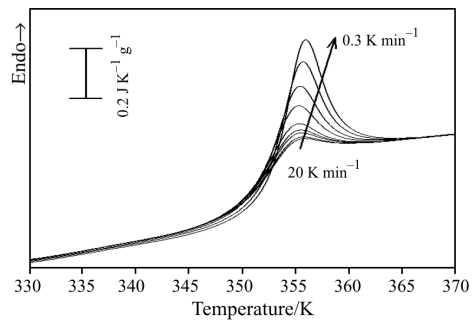


Fig. 4 PET_g-2% MMT: DSC heating curves obtained after various cooling rates (from 20 to 0.3 K min⁻¹ as shown by the arrow), the heating rate is $q^+ = 10$ K min⁻¹

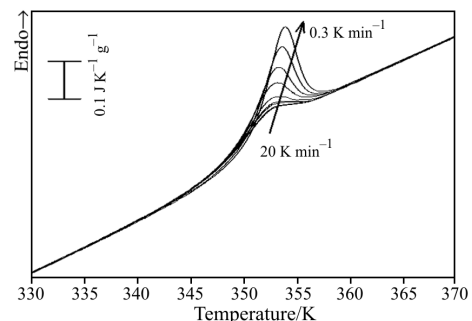


Fig. 5 PET_g-5% MMT: DSC heating curves obtained after various cooling rates (from 20 to 0.3 K min⁻¹ as shown by the arrow), the heating rate is $q^+ = 10$ K min⁻¹

$\Delta C_p(T_g)$ values with MMT content. The average value can be taken equal to 0.26 ± 0.01 J K⁻¹ g⁻¹. For the glass transition temperature T_g , the measured value for PET_g-5% MMT seems smaller than the others. In a first time we can conclude that is not so surprising in regard to other results reported in literature [18–20]. Indeed, it seems that from certain MMT content, the silicate aggregates were not efficiently dispersed or could appear after preparation, inducing a partial phase separation and a lower MMT/PET_g interaction. Consequently, the PET_g chains gain mobility and the glass transition temperature decreases. This phenomenon can be illustrated by Scheme 1a: up to 3% of

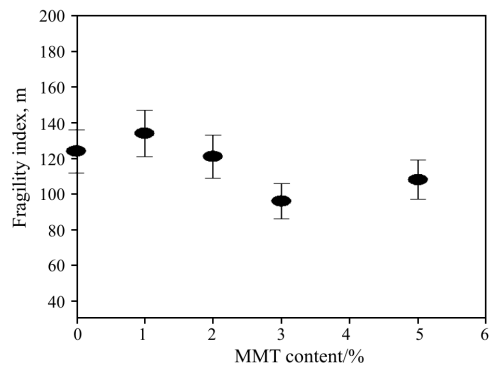


Fig. 6 Variations of the fragility index m determined from Eq. (4) vs. MMT content, the uncertainty corresponding to $m \pm 10\%$

MMT, the mobility of PET_g chains is reduced because of MMT layers. At 5% of MMT, there is partial phase separation and the polymer chains gain mobility. But we can also suppose that the difference between glass transition temperature values is not enough significant and it is then necessary to follow an other quantity evolution in order to conclude, the average size of a CRR for example. In Table 1 we have reported the values of the apparent activation energy $\Delta h^*/R$, and the value of the fragility index m for all the samples, which are plotted vs. the MMT content on Fig. 6. M value slowly decreases up to 3% MMT, but seems to increase for 5% MMT. This result can be discussed from Scheme 1a: up to 3% MMT the amorphous phase formed by PET_g chains is more and more constrained by MMT, involving a decrease of the fragility index. The decrease of the fragility index value when the amorphous phase is more and more constrained has been already observed, for example for semi-crystalline polymers in which the greater the crystallinity the smaller the fragility index m [21]. As for the glass transition temperature behaviour, we suppose a partial phase separation for PET_g-5% MMT sample and then polymer chains gain mobility, involving a more fragile amorphous phase according to the strong-fragile concept. To check this assumption, XED experiments have been carried out on Silicium because this element exists in high quantity in MMT [22]. The Chemical Silicium cartography by XED for PET_g-5% MMT is presented on Fig. 7. The clearest areas correspond to MMT clusters.

This can be better understood from the CRR point of view described in the introduction: from a large panel of polymeric materials scanning a domain of fragility ranging from $m=75$ to 267, we have shown [23] a relationship existing between the fragility index m and the CRR average size at the glass transition temperature $z(T_g)$:

$$z(T_g) \approx m/16 \quad (7)$$

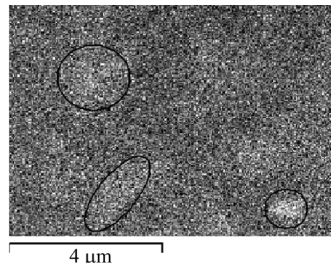


Fig. 7 Chemical silicon cartography by XED for PET_g-5% MMT. The clearest areas correspond to MMT clusters

The so-obtained values $z(T_g)$ (i.e. from DSC measurements) and reported in Table 1, do no evidence any MMT noticeable content dependence. So, $z(T_g)$ is not an enough sensitive parameter to conclude on any change for this sample family.

$z(T_g)$ being a dimensionless quantity, we have chosen to apply the model proposed by Donth *et al.* [25] to give a schematic representation of the CRR evolution in function of MMT content. In this model, the characteristic volume of cooperativity at T_g noted $\xi_{T_g}^3$, and the number of monomer units in the cooperative rearranging region noted N_α , can be estimated from the two following equations:

$$\xi_{T_g} = \frac{\Delta(1/C_v)}{\rho(\delta T)^2} k_B T^2 \quad (8)$$

$$N_\alpha = \frac{\rho N_A \xi_{T_g}^3}{M_0} \quad (9)$$

with N_A the Avogadro number, $(\delta T)^2$ the mean temperature fluctuation related to the dynamic glass transition of one CRR [24–26], T the temperature, k_B the Boltzmann constant, ρ the polymer density (1.27 g cm⁻³ for PET_g), C_v the heat capacity at constant volume and M_0 the molar mass of one monomer unit ($M_0=218$ g mol⁻¹ for PET_g). The approximation for the calculation of the characteristic cooperativity volume $\xi_{T_g}^3$ from Eq. (8) neglects the difference between the heat capacity step at constant pressure and at constant volume and the step of reciprocal specific heat capacity can be estimated from:

$$\Delta(1/C_v) \approx \Delta(1/C_p) = (1/C_p)_{\text{glass}} - (1/C_p)_{\text{liquid}} \quad (10)$$

In this work, the mean temperature fluctuation $(\delta T)^2$ is determined from the experimental curve as proposed by Donth *et al.* [27]: $\delta T = \Delta T / 2.5$ where ΔT is the temperature interval, in which $C_p(T)$ varies from 16 to 84% of the total of ΔC_p step at the glass transition (Fig. 8). Figures 9 and 10 show the evolution of the characteristic cooperativity volume $\xi_{T_g}^3$ and of the monomer unit number in the cooperative rearranging region N_α vs. the MMT content respectively obtained from TMDSC experiments. The uncertainties are in

good agreement with the values given in the literature, i.e. 9% for these two parameters [28]. The number of monomer units per CRR varies approximatively from 100 to 240, and the volume of a CRR varies from 30 to 70 nm³, which corresponds to a cooperativity length of 3.1 to 4.1 nm. These are in good agreement with those obtained on different polymeric materials [28, 29]. It appears very clearly a decrease of the average size (and naturally of the monomer unit number) up to 3% MMT and an increase for the PET_g-5% MMT sample. So, the parameters N_α and $\xi_{T_g}^3$ are more reliable parameters to describe evolution of the cooperative rearranging region size in function of MMT content than the intrinsic parameters as T_g and $\Delta C_p(T_g)$ or the fragility index m . Furthermore, the evolution of N_α and $\xi_{T_g}^3$ parameters vs. MMT content allow us to confirm that, up to 3% the amorphous phase formed by PET_g chains is more and more constrained by MMT, involving a decrease of m , $z(T_g)$, $\xi_{T_g}^3$ and N_α . For PET_g-5% MMT sample, the increase of all these quantities can be explained from cluster formation involving a mobility gain of

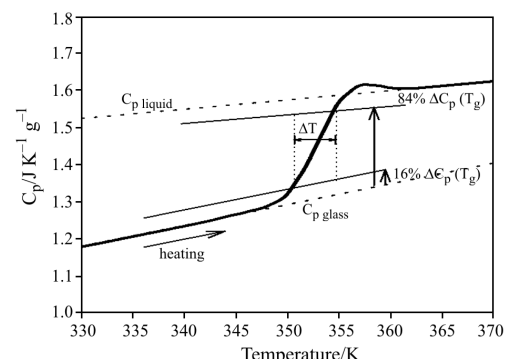


Fig. 8 Example of C_p curve obtained by TMDSC during heating on pure PET_g sample, to explain the determination of the quantities needed for the calculation of the characteristic cooperativity volume at the glass transition $\xi_{T_g}^3$. ΔT is the temperature interval, in which $C_p(T)$ varies from 16 to 84% of the total of ΔC_p step at the glass transition

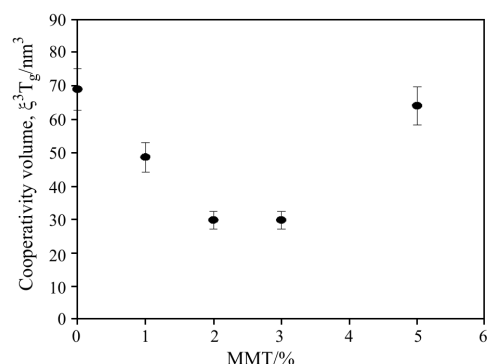


Fig. 9 Evolution of $\xi_{T_g}^3$ – the characteristic cooperativity volume at the glass transition – vs. MMT content. The uncertainty corresponds to $\xi_{T_g}^3 \pm 9\%$

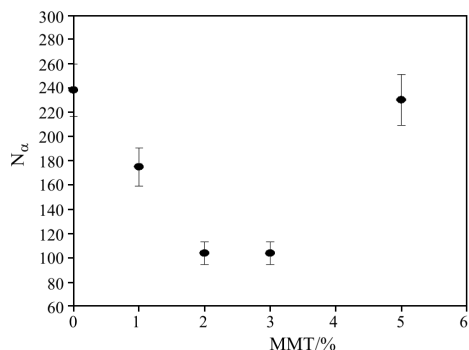
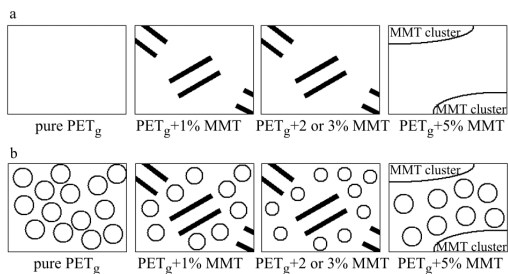


Fig. 10 Evolution of N_α – the number of monomeric units in a cooperative rearranging region – vs. MMT content. The uncertainty corresponds to $N_\alpha \pm 9\%$



Scheme 1 a – Illustration to explain the evolution of PET_g chain mobility vs. MMT content: up to 3% of MMT, the mobility of PET_g chains is reduced because of MMT layers. At 5% of MMT, there is a partial phase separation and the polymer chains gain mobility; b – evolution of CRR size vs. MMT content: up to 3% of MMT, the CRR size decreases. At 5% of MMT, the size is similar to pure PET_g sample: there is partial phase separation and the CRR are not constrained by MMT layers anymore

polymer chains. Then, a new scheme (Scheme 1b) can be drawn to illustrate the behaviour broken from 3% MMT content. Furthermore the fragility index m values obtained from classical DSC measurements and the cooperativity volume values $\xi_{T_g}^3$ obtained from TMDSC measurements give a similar evolution: a decrease up to 3% MMT content and an increase for 5% MMT content. This result is also in good agreement with data collected in literature on polymeric systems [28, 29].

Conclusions

In this work, we have studied the structural relaxation phenomena on PET_g/MMT nanocomposites with different filler contents from DSC and TMDSC investigations. We have determined the glass transition temperature T_g , the specific heat capacity jump $\Delta C_p(T_g)$ and the fragility index m . We have also estimated the average size of a CRR from N_α and $\xi_{T_g}^3$ values, which correspond to the number of monomer units in the cooperative rearranging region and to the characteristic

volume of cooperativity at T_g , respectively. From all these results, we can say that up to 3% MMT the amorphous phase formed by PET_g chains is more and more constrained by MMT, involving a decrease of m , N_α and $\xi_{T_g}^3$. At 5% MMT content, a partial phase separation occurs and the polymer chains gain mobility, involving an increase of m , N_α and $\xi_{T_g}^3$.

References

- 1 L. C. E. Struik, Physical aging in amorphous polymers and others materials, Elsevier, Amsterdam 1978.
- 2 C. A. Angell, Relaxation in complex systems, K. L. Ngai and G. B. Wright, Eds, Naval Research Laboratory, Washington D.C. 1984, p. 3.
- 3 K. L. Ngai, R. W. Rendell, L. D. Pye, W. C. Lacourse and H. J. Stevens, The Physics of Non-Crystalline Solids, Taylor & Francis, London 1992, p. 309.
- 4 A. Q. Tool and C. Eichlin, *J. Am. Ceram. Soc.*, 29 (1931) 276.
- 5 O. S. Narayanaswami, *J. Am. Ceram. Soc.*, 54 (1971) 491.
- 6 C. T. Moynihan, A. J. Eastal, M. A. Debolt and J. Tucker, *J. Am. Ceram. Soc.*, 59 (1976) 12.
- 7 A. Q. Tool, *J. Am. Ceram. Soc.*, 29 (1946) 240.
- 8 G. Bartenev, *Dokl. Akad. Nauk SSSR*, 76 (1951) 227.
- 9 H. N. Ritland, *J. Am. Ceram. Soc.*, 37 (1954) 370.
- 10 H. P. Diogo, S. S. Pinto and J. J. Moura Ramos, *J. Therm. Anal. Cal.*, 83 (2006) 361.
- 11 C. M. Roland and R. Casalini, *J. Therm. Anal. Cal.*, 83 (2006) 87.
- 12 S. H. Glarum, *J. Chem. Phys.*, 33 (1960) 639.
- 13 G. Adam and J. H. Gibbs, *J. Chem. Phys.*, 43 (1965) 139.
- 14 C. A. Solunov, *Eur. Polym. J.*, 35 (1999) 1543.
- 15 M. Alexandre and P. Dubois, *Mater. Sci. Eng.*, 28 (2000) 1.
- 16 Y. Kojima, A. Usuki, M. Kawasumi, Y. Fukushima, A. Okada, T. Kurauchi and O. Kamigaito, *J. Mater. Res.*, 8 (1993) 1185.
- 17 <http://www.nanoclay.com>
- 18 D. Kubies, J. Scudla, R. Puffr, A. Sikora, J. Baldrian, J. Kovárová, M. Slouf and F. Rypásek, *Eur. Polym. J.*, 42 (2006) 888.
- 19 A. Gu and G. Liang, *Polym. Degrad. Stab.*, 80 (2003) 383.
- 20 J. Xiong, Y. Liu, X. Yang and X. Wang, *Polym. Degrad. Stab.*, 86 (2004) 549.
- 21 E. Dargent, E. Bureau, L. Delbreilh, A. Zumailan and J. M. Saiter, *Polymer*, 46 (2005) 3090.
- 22 S. Caillère and S. Hénin, *Minéralogie des argiles*, Masson et Cie 1963.
- 23 A. Saiter, J. M. Saiter and J. Grenet, *Eur. Polym. J.*, 42 (2006) 213.
- 24 E. Donth, *Glasübergang*, Akademie, Berlin 1981.
- 25 E. Donth, *J. Polym. Sci. B*, 34 (1996) 2881.
- 26 E. Donth, *Acta Polym.*, 50 (1999) 240.
- 27 E. Donth, J. Korus, E. Hempel and M. Beiner, *Thermochim. Acta*, 304–305 (1997) 239.
- 28 E. Hempel, G. Hempel, A. Hensel, C. Schick and E. Donth, *J. Phys. Chem. B*, 104 (2000) 2460.
- 29 E. Donth, *The Glass Transition, Relaxation Dynamics in Liquids and Disordered Materials*, Springer, Berlin 2001.